

SPECTRAL ANALYSIS OF LUNAR CINDER CONES IN THE MARIUS HILLS VOLCANIC COMPLEX

M. J. McBride¹ B.H.N. Horgan¹ and S. J. Lawrence², ¹Purdue University, 610 Purdue Mall, West Lafayette, IN 47907 (mjmcbride@purdue.edu). ²NASA Johnson Space Center (mjmcbride@purdue.edu).

Introduction: Within the Oceanus Procellarum on the near-side of the Moon, the Marius Hills Volcanic Complex (MHVC) is located at 13.3°N, 47.5°W (Fig 1).

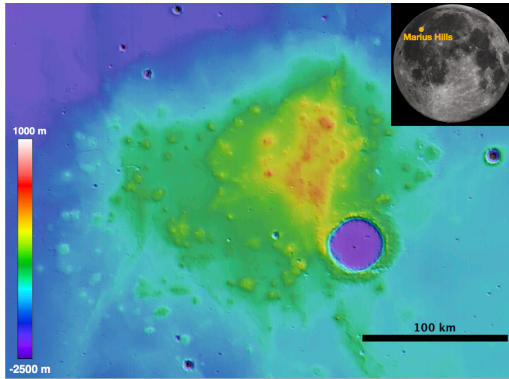


Figure 1: A) Location of MHVC on the near side of the Moon. B) Topography of the MHVC from the LOLA data.

The MHVC is a 35,000 km² plateau raised 100-200 m from the surrounding plains, known for having a wide assortment and concentration of volcanic features [1,2]. These volcanic features include volcanic domes, lava flows, sinuous rilles, and volcanic cones.

The volcanic cones in the MHVC were identified initially using visible imagery and the known morphologies associated with cinder cones on Earth [2, 13]. A definitive designation of a cinder cone would require evidence that the volcanic edifice was constructed of ballistic pyroclasts from an explosive, volatile-rich eruption. An explosive, volatile-rich eruption produces rapidly quenched, glassy, pyroclasts as represented by cinders on Earth. It is expected that the same process would occur on the lunar surface within the MHVC. Therefore, the driving questions behind this research are: Do the conical structures in the MHVC have a spectral signature associated with the presence of glass? And, is it possible to use mineralogy to indicate the presence of a volcanic cone where visible imagery is ambiguous?

Background: Photogeologic and compositional analyses have previously characterized the geologic units within the MHVC. The region has been studied using images from the LRO NAC [3, 4], 9-band spectral data from Clementine [3, 8], and compositional analyses using data from the Moon Mineralogy Mapper [M³;8,9,10]. A previous, M³ analysis was not able to spectrally distinguish the volcanic cones from the surrounding terrain and revealed an abundance of olivine in the MHVC [9]. The identification of olivine, a primitive

mineral that is thought to have originated at depth within the lunar crust, has been problematic on the lunar surface because it is difficult to distinguish from volcanic glass in planetary spectral analyses [6]. The combination of spectral indices used here [6] can differentiate olivine from volcanic glass in M³ data.

Lawrence *et al.* (2013) used the Lunar Reconnaissance Orbiter Wide and Narrow Angle Cameras to complete a morphological survey of the cinder cones of the MHVC. A total of 93 cinder cones were identified and characterized by their shape into three categories: C-class, E-class, and N-class. 64 cones were designated C-class because of their C-shape, potentially due to a collapse of the cinder cone wall due to a late-stage effusive lava flow. E-class cones otherwise known as elongated shaped cones are formed from fissure eruptions and also have a gap attributed to lava flows. E-class cones account for 12 cones in the MHVC. The 17 cinder cones that are entirely circular and do not exhibit a gap were designated N-class cones. In addition to the 93 cones that were classified by Lawrence *et al.* (2013), there were 55 circular structures could not be definitively designated cones and were classified as U-class. The cone type and the location are plotted on the map in Figure 2.

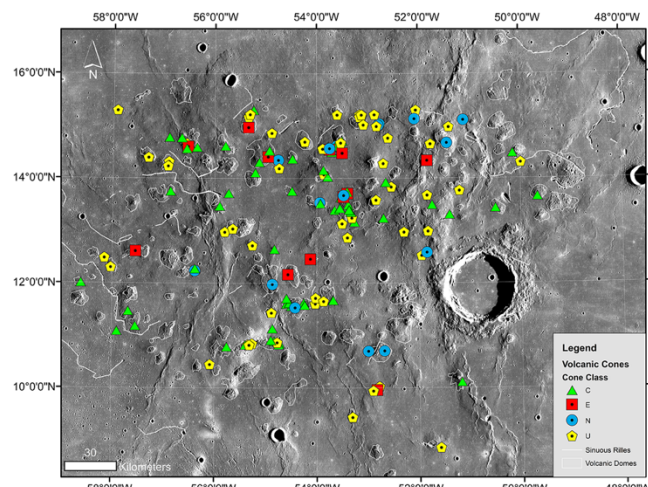


Figure 2: Lawrence *et al.* (2013) image of the MHVC with the location of volcanic cones characterized by shapes and the location of the candidate volcanic cones.

Methods: M³ was an imaging spectrometer on the Chandrayaan-1 lunar orbiter operating in the visible to near-infrared (0.42μm-3.0μm). M³ in global mode has a resolution of 140 m/pixel in 86 spectral channels [11]. M³ collected data during two operational periods distin-

guished by changes in instrument temperature and viewing orientation. Data in this project was obtained from operational periods 1B, 2A, 2B, and 2C. A M^3 map of the region was constructed with bounds 300-312°E and 9-17°N. The continuum of each spectrum was removed [6, 7] using a linear convex hull with two segments between 0.6-2.6 μm . Spectral noise was reduced using a median filter and a boxcar smoothing algorithm, both with widths of 5 channels.

Spectral parameters were applied to our M^3 map. Our glass spectral parameter detects the wings of the glass iron absorption band, which is centered at much longer wavelengths than other Fe-bearing minerals, based on the average band depth below the continuum at 1.15, 1.18, and 1.20 μm [14]. Figure 3 shows these maps along with topography from LOLA.

Preliminary Results: Using the M^3 data, some of the volcanic cones within the MHVC have already been evaluated. Figure 3 displays three examples of LROC

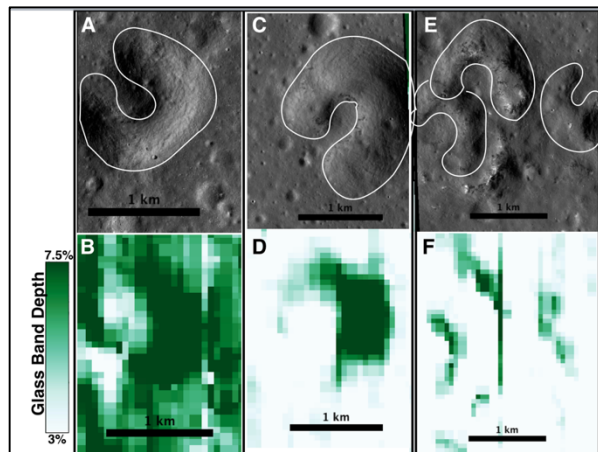


Figure 3: LRO Narrow Angle Camera (NAC) views and M^3 derived glass band depth maps for several cinder cones at MHVC. The cinder cone morphologies can be seen in the associated glass maps as would be expected for cinder cones.

NAC images displaying known volcanic cones. Below the LROC images, are the associated spectral glass parameter maps [16]. In the glass parameter maps, the shape and orientation of the volcanic cones mirror the visible imagery. The matching shapes do indicate that the volcanic cones are glass-rich as expected in an explosive eruption resulting in cinders. Preliminary investigation of U-class cone locations reveals the presence of increased glass band signature indicative of the positive relief feature being a cinder cone instead of a mantled impact crater, degraded lava flow front, or other lunar geologic feature [4].

In addition to the mapping of the spectral parameters, individual spectra were collected from confirmed cinder cones. As seen in Figure 4, the spectra display

characteristic bands associated with glass-rich mineralogy. When comparing the location of the broad 2 μm band to the laboratory spectra also included in Figure 4, it is possible to see the influence of basaltic glass in the cone composition. The glass-rich spectral signature of the cinder cone is unique compared to the surrounding orthopyroxene-rich volcanic domes and mare [16].

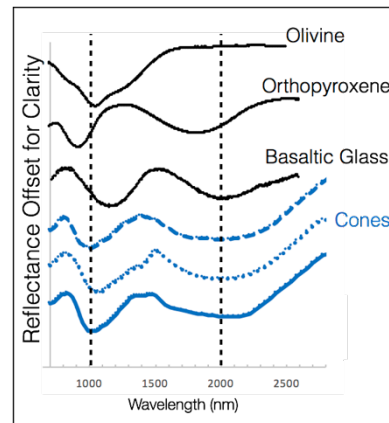


Figure 4: Spectra of volcanic cones in blue are compared to laboratory spectra of olivine, orthopyroxene, and basaltic glass in black.

Summary and Future Work: Lawrence *et al.* (2013) developed a comprehensive list of the location and types of cinder cones in the MHVC. The goal of this research is to map and identify these cones in the M^3 spectral data while analyzing for trends related to cinder cone shape or location. The list of 55 U-class potential cones will be evaluated to determine if the presence of glass could prove or disprove the designation of volcanic cinder cone where LROC imagery was inconclusive. In the years since the Lawrence *et al.* (2013) survey, there has been more LROC data collected. Therefore, the number of the unidentified cones could surpass the 55 U-class cones. Using spectral data in the MHVC can increase known amount and the extent of volcanic cones which require a higher volatile contribution for formation than the other volcanic features in the region.

References: [1] Whitford-Stark and Head (1977), LPSC, 8th, 2705-2724. [2] McCauley 1967, McCauley, J. F., U.S. Geol. Surv. Misc. Invest. [3] Gustafson *et al.*, (2012), J. Geophys. Res. Planets, 116(E6), E00G13 [4] Lawrence *et al.*, (2013), J. Geophys. Res. Planets, 118, 615-634. [5] Gaddis, L.R. *et al.* (2003) Icarus, 161:2, 262-280. [6] Horgan *et al.*, 2014, Icarus, 234(C), 132-154. [7] Bennett *et al.* (2016) Icarus, 273, 296-314. [8] Weitz *et al.*, (1999), J. Geophys. Res. Planets, 104(E8), 18933-18956. [9] Besse *et al.*, (2011), J. Geophys. Res. Planets, 116, E00G13. [10] Heather *et al.*, (2003), J. Geophys. Res. Planets, 108(E3), 5017 [11] Pieters, C. M. *et al.* (2009) Curr. Sci, 96:4, 500-505 [12] McBride *et al.* (2016) LPSC, 47, 3052. [13] Wood (1979) LPSC, 10, 1370. [14] Gaddis *et al.* (2016), LPSC, 47, 2065. [15] Spudis *et al.*, (2013), J. Geophys. Res, 118, 1-19. [16] McBride *et al.*, (2017), LPSC, 48, 2989.